



HAL
open science

Influence of the initial water content in flash calcined metakaolin-based geopolymer

Raphaëlle Pouhet, Martin Cyr, Raphaël Bucher

► **To cite this version:**

Raphaëlle Pouhet, Martin Cyr, Raphaël Bucher. Influence of the initial water content in flash calcined metakaolin-based geopolymer. *Construction and Building Materials*, 2019, 201, pp.421-429. 10.1016/j.conbuildmat.2018.12.201 . hal-02395947

HAL Id: hal-02395947

<https://hal.insa-toulouse.fr/hal-02395947>

Submitted on 12 Oct 2021

HAL is a multi-disciplinary open access archive for the deposit and dissemination of scientific research documents, whether they are published or not. The documents may come from teaching and research institutions in France or abroad, or from public or private research centers.

L'archive ouverte pluridisciplinaire **HAL**, est destinée au dépôt et à la diffusion de documents scientifiques de niveau recherche, publiés ou non, émanant des établissements d'enseignement et de recherche français ou étrangers, des laboratoires publics ou privés.

1 **Influence of the initial water content in flash calcined**
2 **metakaolin-based geopolymer**

3
4 POUHET Raphaëlle, CYR Martin, BUCHER Raphaël

5 ^{1,2}, Université de Toulouse, LMDC, INSA/UPS Génie Civil, 135 Avenue de Rangueil, 31077
6 Toulouse cedex 04 France.

7 pouhet@insa-toulouse.fr, martin.cyr@insa-toulouse.fr, bucher@insa-toulouse.fr

8 **Keywords:** Geopolymer, Metakaolin, water content, compressive strength, porous network,
9 transfer properties.

10
11
12 **Abstract.**

13 This study assesses the influence of the initial amount of water in metakaolin-based
14 geopolymer on some of its properties in the hardened state. Results suggest a linearly
15 decreasing influence of the amount of water on the mechanical performance of the
16 geopolymer and showed that the majority of this water was not bonded to the structure.
17 Moreover, it was found that whatever the amount of water initially introduced, all the samples
18 contained the same amount of water after a drying period. The study of the porous network
19 showed a large pore volume of 50% of the total volume which corresponds to the volume of
20 water initially introduced. Finally, the observation of numerous macropore helped to explain
21 the high transfer coefficients measured on the geopolymer.

1. Introduction

The evolution of knowledge on alkali activated materials (AAM) and, more specifically, on geopolymers (GP), tends to show that they could provide an efficient alternative to ordinary Portland cement (OPC) (Shi et al., 2006; Provis et al., 2009a; Bligh et al., 2013; Pacheco-Torgal et al., 2014; Palomo et al., 2014). Geopolymers are aluminosilicate materials formed by the activation of an aluminosilicate source, such as metakaolin, by a strongly basic alkaline solution. This results in the formation of amorphous materials at room temperature (Duxson et al., 2007a), showing compressive strength comparable to that of a traditional hydraulic binder (Pouhet and Cyr, 2016a). For the geopolymer the Water/Cement mass ratio is not much used in the literature, as it could be for OPC. However, without necessarily anticipating the consequences that it can have on the hardened state of the material, it is easy to see that the amount of water introduced can be very important. The purpose of this study is to anticipate the performance of a metakaolin-based geopolymer by studying the influence of the proportion of water initially introduced into the mixture.

The silica, aluminium, alkali and water brought to the geopolymer mixture by the raw materials are mentioned in the literature in the form of three molar ratios, which fix the total formulation of a geopolymer: SiO_2/Al_2O_3 , Na_2O/Al_2O_3 and H_2O/Na_2O . The main issue with the use of these ratios is that the variation of any one of them induces a variation of the total quantity of water in the mixture. Thus it is often difficult to distinguish the influence of just the initial amount of water on the parameters studied. Some authors use special molar ratios to define the total amount of water in the formulation: $H_2O/(SiO_2+Al_2O_3)$, H_2O/R (some use H_2O/R_2O , $R=Na$ or K) or H_2O/Al_2O_3 (Lizcano et al., 2012; Perera et al., 2005; and Okada et al., 2009, respectively) but that implies that the other molar ratios have already been set. Other authors use a “Liquid-to-solid” or Water-to-solid” mass ratio (Álvarez-Ayuso et al., 2008; Provis et al., 2009b; Zuhua et al., 2009; Zang et al., 2010; Park and Pour-Ghaz, 2018). However, this is not always defined in the same way due to the fact that the activation solution is liquid but contains sodium and silica. Sometimes the ratio corresponds to the mass of activating solution over the aluminosilicate mass (Álvarez-Ayuso et al., 2008; Provis et al.,

50 2009a), sometimes it is the total mass of water over the sum of all the solid components
51 introduced into the mix (Pouhet and Cyr, 2016a), and sometimes it is used without being
52 defined (Zang et al., 2010; Zuhua et al., 2009).

53 The impact of the molar ratios on the hardened state of metakaolin-based geopolymer is now
54 widely referenced in the literature regarding their mechanical performances (Kamalloo et al.,
55 2010; Rowles et al., 2003; Duxson et al., 2007b), microstructures (Duxson et al., 2005;
56 Barbosa, 2000), and porous networks (Duxson, 2005; Steins et al., 2013) but very few studies
57 discuss the influence of the initial amount of water introduced into the mixture on the
58 hardened state of geopolymer, independently of the other components (Zuhua et al., 2009;
59 Okada et al., 2009; Lizcano et al., 2012). Among these authors, Lizcano et al. assessed the
60 effects of chemistry, and curing and ageing conditions on water loss kinetics, porosity, and the
61 structure of metakaolin-based geopolymers (Lizcano et al.; 2012). Their results showed that
62 the initial amount of water was the dominant factor affecting the density and the open porosity
63 of geopolymers after curing and extended ageing. This study also showed that whatever the
64 amount of water introduced initially, after 21 days in open moulds at 20 °C and around 74 %
65 R.H., all specimens had a final water content of around 15% to 20% (for geopolymer
66 activated by sodium). Finally, the authors demonstrated a strong correlation between the
67 initial water content and the open porosity of the geopolymer. Okada et al. (Okada et al.,
68 2009) obtained similar results on metakaolin-based geopolymer, showing that the increase in
69 the initial water content increased both the size and the volume of the porous network. Perera
70 et al. (Perera et al, 2005) showed that water was present in the geopolymer in three forms: 1-
71 “free water” (or intergranular water), which is removed between room temperature and 150
72 °C; 2- water removed between 150 °C and 300 °C, which would correspond to the “interstitial
73 water”; and 3- water related to OH⁻ groups bound into the structure of new-formed products,
74 representing only very small amount of water measured between 300 °C and 700 °C (Perera
75 et al., 2005). White et al. (White et al, 2010) used neutron pair distribution function (PDF) to
76 improve their understanding of the local atomic structural characteristics of geopolymer
77 binders derived from metakaolin, specifically the nature and amount of the water associated

78 with these materials. Their findings were consistent with those of previous studies, showing
79 that only small amounts of water (<5% for geopolymer activated by potassium) may exist in
80 small pores and as terminal hydroxyl groups in the Si–Al framework structure. Most of the
81 water is lost below 200 °C, indicating that it is mainly found in large pores or hydrating the
82 charge-balancing cations associated with the Si–Al framework.

83 The above mentioned studies provide some important information about the organization of
84 the water in the hardened metakaolin-based geopolymer, but none of them addresses the
85 consequences of this presence of water. This study therefore proposes an investigation into
86 the influence that the initial water content in metakaolin-based geopolymer has on the
87 hardened state, in the aim of being able to anticipate the final behaviour of the material in
88 terms of mechanical performance and transfer properties.

89

90 **2. Materials and methods**

91 **2.1. Geopolymer raw materials and synthesis**

92 The source of aluminosilicate was a metakaolin obtained by flash calcination, produced in the
93 south west of France by ARGECO Développement. The term "flash calcination" refers to the
94 combustion process where the particles of kaolinite are transformed into metakaolin by
95 passing near a flame for a few tenths of a second (temperature around 700 °C) (San Nicolas,
96 2013). Table 1 presents the mass content of oxides in the flash metakaolin, obtained by ICP-
97 OES, using an Optima™ 7000 DV ICP-OES (PerkinElmer) equipped with a CCD sensor.
98 These results show very large silica content, mainly due to the presence of quartz in the raw
99 kaolin, confirmed by XRD analyses. However, after quantification, only the amorphous part
100 of this silica (around 29% of the metakaolin mass) was taken into account in the formulation
101 of the geopolymer. The specific surface area of the flash metakaolin was 13 m²/g (BET). The
102 activating solution used was an industrial sodium silicate solution (Bétol 49T, Woellner)
103 containing 8 % Na₂O by mass and having an SiO₂/Na₂O ratio of 3.3 (Table 1). In order to
104 adjust the sodium content, pure-grade NaOH was added to this commercial solution 24 h
105 before the geopolymer preparation. This initial solution had a high water content (65.6 wt%,

106 Table 1), so a moderate evaporation of a certain amount of water, performed at low
 107 temperature 24 h before the preparation, was necessary for some geopolymers.

108

109 **Table 1.** Mass composition of raw materials.

	SiO ₂	Al ₂ O ₃	CaO	MgO	Fe ₂ O ₃	K ₂ O	Na ₂ O	TiO ₂	SO ₃	H ₂ O
Flash metakaolin	68.10	24.10	0.91	0.22	3.73	0.35	0.08	1.14	0.03	-
Waterglass solution	26.5	-	-	-	-	-	8.0	-	-	65.6

110

111 The geopolymer was prepared in two steps. First, pure NaOH and water were added to the
 112 industrial waterglass solution to obtain the desired SiO₂/Na₂O and H₂O/Na₂O molar ratios.
 113 After total dissolution of the sodium hydroxide, the solution was cooled to 20 °C for 24 h and
 114 then mixed with the metakaolin until the mixture was homogeneous.

115 The geopolymer mortars were mixed and made according to French standard EN 196-1 in a 5
 116 L mixer (Automix, Controls[®]), using the activation solution instead of the mixing water. The
 117 formulations are presented in Table 2. Standard sand (EN 196-1 and ISO 679: 2009 standards)
 118 composed of well crystallized quartz and having a controlled particle size between 0 and 2
 119 mm was used. The mortar specimens were cast in 4 x 4 x 16 cm moulds using a shock table,
 120 and pastes were cast in 7 x 4.3 x 2.2 cm plastic prisms. All specimens were cured at 20 °C in
 121 sealed bags for the first 24 hours and then demoulded and stored at 20 °C and 95 % R.H. until
 122 testing.

123

124 **Table 2.** Mass composition of geopolymer (solid molar composition: 3.6SiO₂•1Al₂O₃•0.9Na₂O)

Sample ID	Mk (g)	Silicate (g)	NaOH (g)	H ₂ O (g)	Sand (g)	Water in GP (wt.%)	Water/solid
GP0.38	450	372	37.8	-12.1*	1350	27%	0.38
GP0.4	450	372	37.8	5	1350	29%	0.40
GP0.5	450	372	37.8	65.1	1350	33%	0.50
GP0.6	450	372	37.8	125.1	1350	37%	0.60
GP0.7	450	372	37.8	185.1	1350	41%	0.70

125 * negative value corresponding to the mass of water evaporated from the alkali silicate solution.

126

127 **2.2. Test methods**

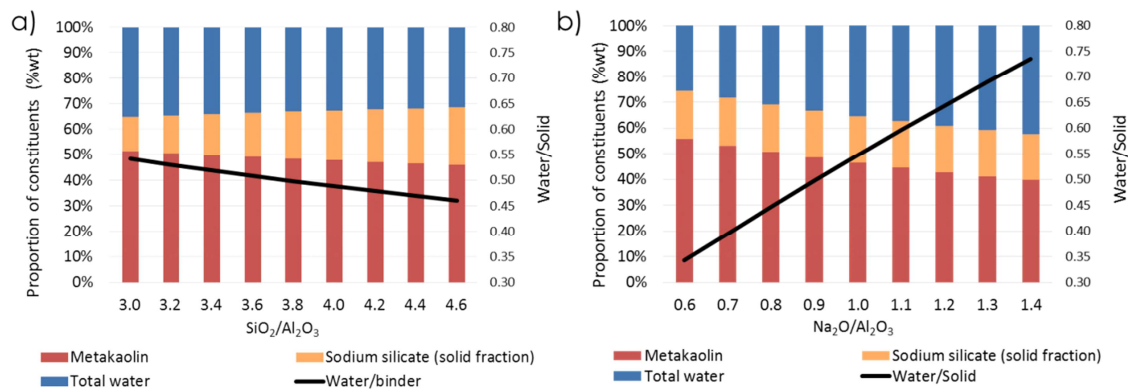
128 The mechanical tests in flexion and compression were performed on 3 prismatic mortar
129 specimens of dimensions 4 x 4 x 16 cm, according to EN 196-1 (Automatic mortar press,
130 Class A - 3R[®] RP30/200FP). The mineralogical study was carried out by X-ray diffraction
131 (XRD) using a Bruker D8 Advance diffractometer, with Bragg-Brentano configuration and
132 copper radiation (Cu K α , $\lambda = 1,5406\text{\AA}$). The acquisitions were made on powder having a
133 maximum particle size of 80 μm , between 5° and 70° 2 θ , with a step size of 0.02° and an
134 acquisition time of 1.075 seconds per step. The total pore volume was determined in this
135 study by measuring the porosity accessible to water via the French standard NF P18-459
136 (2010). Tests were carried out on at least three 7 x 4.3 x 2.2 cm prisms of geopolymer paste.
137 The balance accuracy for the mass measurements was 0.001g. Mercury intrusion porosimetry
138 measurements (MIP) were performed with a Pascal 140 porosimeter coupled with a Pascal
139 240 (Fusion Instrument) and the samples analysed were pieces of paste of around 1 g obtained
140 by fresh fracture at 7 days. Gas absorption/desorption analyses were performed using a Tristar
141 3020 apparatus (Micromeritics), with a degassing temperature of 100 °C, on a geopolymer
142 paste piece prepared in the same way as those studied by mercury porosimetry. X-ray
143 microtomography images were obtained with a Nanotom 180 from Phoenix / GE. The
144 acquisition parameters used were a voltage of 80 kV and an intensity of 100 μA . The
145 resolution obtained for this type of sample was a 5.4 micron voxel. The volumes were rebuilt
146 using the Datos X software (Phoenix) and VG Studio Max (Volume Graphic) to obtain an
147 image of the porosity of the material. Finally, cross-sections of 100 day old geopolymer were
148 observed by scanning electron microscopy (SEM) after application of a focused ion beam
149 (FIB) apparatus (FEI Helios NanoLab 600i). FIB uses Ga⁺ ions to remove material with a
150 very high spatial precision. In this way, cross-sections of a representative sampling area were
151 obtained at a specific location after surface observation. For this operation, the sample was
152 positioned in the SEM chamber, tilted at 52° and a 2 micron thick layer of platinum (Pt) was
153 laid down for surface protection. FIB milling was then applied to etch the sample.

154

155 3. Results and discussion

156 3.1. Influence of water content on mechanical performance

157 Using three molar ratios (SiO_2/Al_2O_3 , Na_2O/Al_2O_3 and H_2O/Na_2O) to formulate the
158 geopolymer led to a systematic variation of the water content, as illustrated in Figure 1.
159 Increasing the SiO_2/Al_2O_3 ratio decreased the amount of water in the formulation. Conversely
160 increasing the Na_2O/Al_2O_3 or the H_2O/Na_2O ratios increased the total water content.



161

162

163 **Figure 1.** Examples of evolution of the proportions of the geopolymer constituents (MK + sodium silicate (solid
164 fraction) + total water) and the Water/Solid mass ratio depending on a) SiO_2/Al_2O_3 and b) Na_2O/Al_2O_3 molar
165 ratios, the other two molar ratios being kept constant (including H_2O/Na_2O).

166

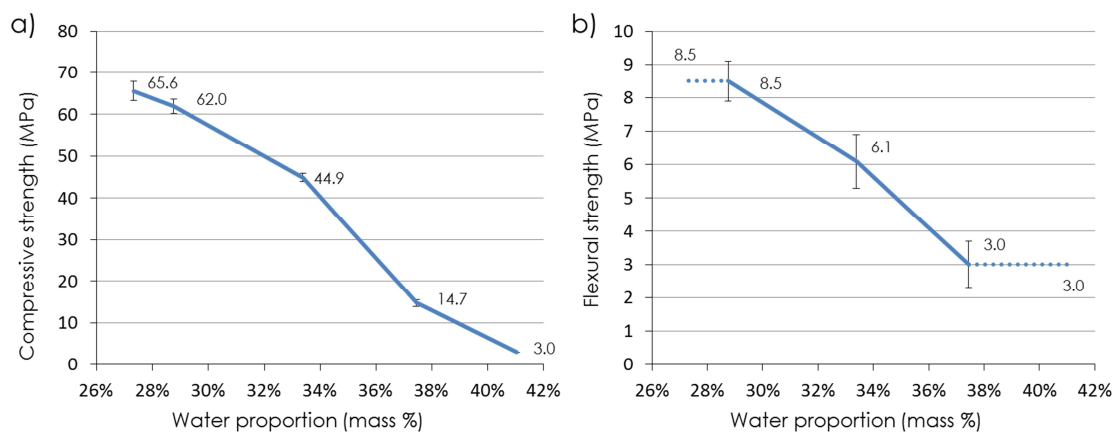
167 In this study, we chose to work around these ratios and clearly dissociate the solid from the
168 liquid. Thus only two parameters had to be fixed:

- 169 - The geopolymer molar formulation, corresponding to the solid part initially introduced
170 and written in the form $xSiO_2 \cdot yAl_2O_3 \cdot zNa_2O$.
- 171 - The amount of water introduced, written in the form of the water content (mass
172 percentage) or the Water/Solid mass ratio.

173

174 The formulation of the metakaolin-based geopolymer was the subject of an earlier study,
175 which highlighted an optimal proportion regarding the mechanical performances
176 corresponding to the initial composition: $3.6SiO_2 \cdot 1Al_2O_3 \cdot 0.9Na_2O$ (Pouhet, 2015).

177 To assess the influence of the water content on the mechanical performance, five geopolymer
 178 mortars with increasing amounts of water were tested in flexural and compressive strength.
 179 The corresponding formulations are listed in Table 2. Given that the waterglass solution
 180 provided large quantities of water in addition to silica and sodium, one formulation, GP0.38,
 181 required an additional step during its preparation. The significant water contribution of the
 182 activation solution (65.5%) made it impossible to obtain formulations having a Water/Solid
 183 mass ratio lower than 0.4. Excess water was therefore removed from the waterglass solution
 184 by evaporation 24 h before the mortar preparation, by heating at 50 °C under agitation until a
 185 loss of mass equal to the required amount of water was achieved. No visual modification was
 186 observed on the remaining solution. The results of the mechanical tests (performed in
 187 compression and in bending) on the five mortars of Table 2 are presented in Figure 2.



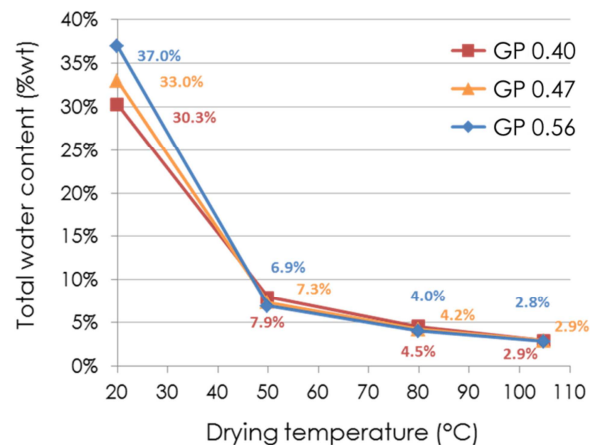
188
 189 **Figure 2.** a) Compressive and b) Flexural strengths of geopolymer mortars at 7 days depending on the water
 190 proportion introduced in the initial mixture (Solid formulation: $3.6 \text{ SiO}_2 \cdot 1 \text{ Al}_2\text{O}_3 \cdot 0.9 \text{ Na}_2\text{O}$)
 191

192 Plotting the measured strengths as a function of the proportion of water in the mixture showed
 193 the same trends in flexion and compression. It was observed that, between water proportions
 194 of 28% and 37%, increasing the amount of water decreased the mechanical performance (only
 195 between 29% and 37% in the case of the flexural strength). In view of these figures, it would
 196 seem that the mechanical performance of the geopolymers would follow a linear trend with a
 197 decrease in mechanical strength proportional to the initial amount of water, at least in the W/S
 198 domain studied. This result therefore demonstrates a different behaviour that observed for
 199 cement witch shows a non-linear decrease in performance with the addition of water (e.g.

200 Bolomey). Furthermore, this observation is in agreement with the literature, which postulates
201 that the introduced water is not used for the formation of hydrate as in Portland cement
202 (Perera et al., 2005, White et al., 2010), and therefore does not participate in the structuration
203 of the material. Thus the addition of water in a geopolymer formulation systematically entails
204 a weakening of the material, probably by increasing the porosity.

205 3.2. Investigation on the bound water

206 The literature shows that, in the hardened geopolymer, the water does not appear to be bound
207 in the network in hydrate form as it is in cement matrix (Barbosa et al., 2000; Lizcano et al.,
208 2012; White et al., 2010; Perera et al., 2005). Thus, determining the fate of the water in the
209 hardened geopolymer paste is indispensable for a better understanding of its influence. It was
210 therefore decided to study the amount of water that could be removed by drying the
211 specimens at relatively moderate temperature, in order to observe the influence on the
212 mechanical performances. Three water contents were chosen, corresponding to W/S ratios of
213 0.40, 0.47 and 0.56, with three drying temperatures of 50 °C, 80 °C and 105 °C. After
214 stabilization of the mass loss for each drying temperature, the amount of water remaining in
215 the geopolymer was calculated.



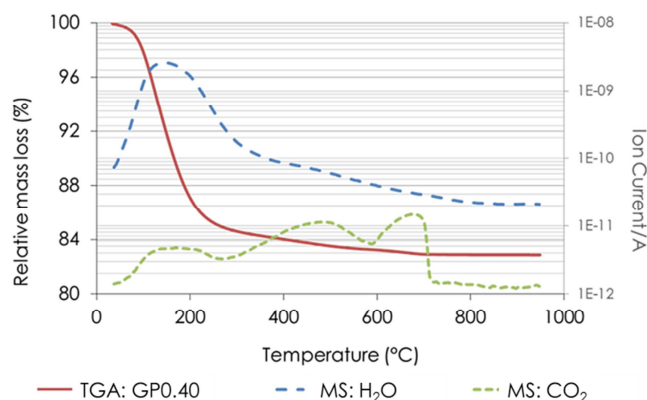
216

217 *Figure 3. Evolution of the total amount of water in GP0.40, GP0.47 and GP0.56 depending on the drying*
218 *temperature.*

219 Total water contents of the geopolymers for the three W/S ratios according to the drying
220 temperature are presented in Figure 3. The figure clearly shows that, whatever the initial
221 water content in the geopolymer paste, this content was reduced to about 3% for all the

222 formulations after drying at 105 °C, which corresponds to a relative loss of 90-92% of the
223 initial water mass. The evolution of the water content in geopolymer versus the drying
224 temperature tended to an asymptotic value above 105 °C, suggesting a slower evolution for
225 the loss of the 10% remaining water.

226 In order to visualize the temperature at which the remaining water evaporates, TGA analysis
227 was carried out on the GP0.40, coupled with mass spectroscopy. The results obtained are
228 presented in Figure 4. According to the TGA result, evaporation of the remaining water would
229 be a long process, as traces of water were still measured at 700 °C. This could indicate that a
230 small proportion of the water initially introduced remained in small pores or as terminal
231 hydroxyl groups in the structure and that this quantity of water would be the same regardless
232 of the initial amount of water introduced, as described in the literature (Perera et al., 2005;
233 White et al., 2010). At the end, the total molar formulation calculated by considering the
234 water “fixed” to the structure (therefore not evaporated at 105 °C) was nearly the same for the
235 three formulations and corresponded to $3.6 \text{ SiO}_2 \cdot 1 \text{ Al}_2\text{O}_3 \cdot 0.9 \text{ Na}_2\text{O} \cdot 1.3 \text{ H}_2\text{O}$. The
236 presence of carbon dioxide in the mass spectroscopy spectrum means that carbonation took
237 place during the seven days of curing, which is consistent with results obtained in a previous
238 study (Pouhet and Cyr. 2016b).



239

240 **Figure 4.** Thermogravimetric analysis of geopolymer GP0.40 at 7 days performed at 20.0 °C/min up to 950 °C
241 with H₂O and CO₂ mass spectroscopy spectrum.

242

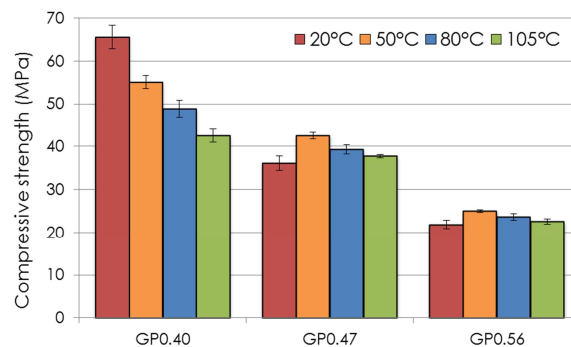
243 In order to confirm that the departure of this "free water" was not detrimental to the
244 geopolymer structure, the same drying protocol was applied to GP0.40, GP0.47 and GP0.56

245 geopolymer mortars, which were then tested in compression. As previously, the geopolymers
246 were kept without external exchanges for seven days and then placed in a climatic chamber
247 until stabilization of the mass loss. Figure 5 presents the compressive strengths measured
248 according to the drying temperature for the three W/S ratios studied. Two behaviours can be
249 observed:

- 250 - The formulation having the least water, GP0.40, showed a loss of strength that was
251 moderate but increased with increasing drying temperature.
- 252 - The GP0.47 and GP0.56 formulations showed similar behaviour, with very close
253 compressive strength values regardless of the applied temperature.

254 Some hypotheses can be advanced to explain the behaviours observed. It was measured that
255 about 90% of the introduced water was evaporated between 20 °C and 105 °C. The fact that
256 the mechanical performances of the GP0.47 and GP0.56 formulations did not change between
257 these two temperatures could validate the assumption that it was indeed "free water" and
258 therefore not related to the structure and its stiffness. In view of the above results, it is highly
259 probable that this was also the case for the GP0.40 formulation despite the loss of strength.
260 However, for this formulation having the lowest water content, the loss of strength observed
261 could have been due to a difference in the organization of the porous network containing this
262 "free water". In this case, the porosity could have been finer or arranged differently, so that
263 the evaporation of the "free water" would lead to damage in the material and therefore to a
264 decrease in mechanical performance.

265



266

267 **Figure 5.** Compressive strength of geopolymer mortars at 7 days performed after mass loss stabilization

268

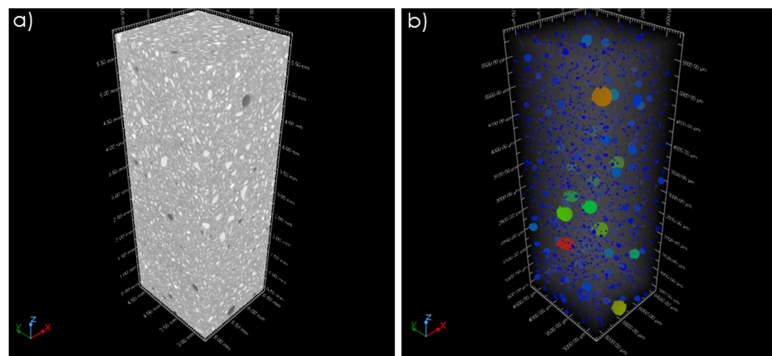
depending on the drying temperatures for three different Water/Solid mass ratios.

269 **3.3 Influence of the water content on the volume and organization of**
270 **the porous network of geopolymers**

271

272 In this study the intention was to characterize all of the water in the geopolymer. So it was
273 firstly necessary to evaluate the size and organization of the water present in the air bubbles
274 trapped during preparation. GP0.40 geopolymer paste prepared without any shocks or
275 vibration was analysed by X-ray tomography to visualise the air occlusions, assess their size
276 distributions and quantify their cumulative volume. A 3D section of the sample, having
277 dimensions 2 x 2 x 5 mm was isolated and analysed. Figure 6a presents the 3D section,
278 showing the overall sample and the air occlusions, which were easily identified by their dark
279 coloration. Using this strong contrast between the air and the matrix allowed the software to
280 isolate this volume and to represent it separately. Figure 6b, which isolates the entrapped air
281 fraction, shows significant numbers of spheres with diameters ranging from 40 μm up to
282 nearly 300 μm . It was calculated that this cumulative volume represented 2% of the sample.
283 The distribution of the sphere sizes is illustrated by different colours: the blue corresponds to
284 diameters smaller than 200 μm , with decreasing diameters shown in darker shades of blue,
285 while all other colours correspond to diameters ranging from 200 μm to 300 μm . Figure 6b
286 shows a homogeneous distribution of the bubbles in the sample with no privileged
287 organization. However, the result does not show if there is an interconnectivity of the
288 porosity, which would be too fine for the resolution of the device.

289



290

291

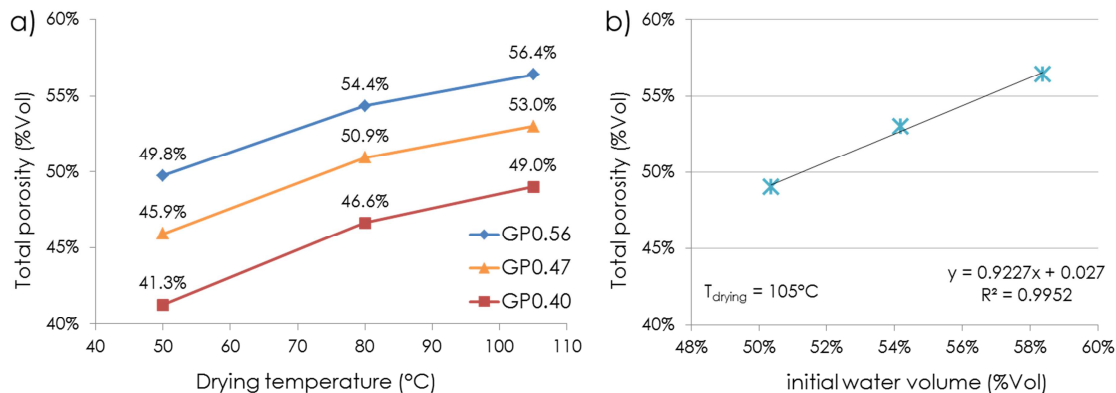
292

Figure 6. X-ray tomography visualization of G0.40 paste showing: a) 3D section of the sample and b) the same 3D section presenting only the air occlusions.

293 To define the porosity of the geopolymer and the influence of the initial water content, the
 294 total porosity accessible to water was measured (NF P18-459) and mercury intrusion
 295 porosimetry (MIP) was performed on geopolymer specimens having three different W/S mass
 296 ratios. Figure 7a shows the porosity accessible to water measured using the same three drying
 297 temperatures as those used for the study of the bonded water.

298 The information obtained as described in the previous two paragraphs showed that, for the
 299 GP0.47 and GP0.56 formulations, the temperature of 105 °C caused no loss of strength and
 300 led to final water contents close to 3%. Thus, the total porosity values measured for these
 301 formulations with a drying temperature of 105 °C was very probably close to the total
 302 porosity values of the materials, i.e. 53.0% and 56.4% respectively. Since the drying
 303 behaviour of the three formulations was similar (Figure 7a), it seems reasonable to conclude
 304 that, despite the loss of mechanical strength, the total porosity of the GP0.40 formulation can
 305 be measured by drying at 105 °C and so would be 49%. This value is in agreement with
 306 values found in the literature for similar formulations (Boher, 2014).

307



308

309 **Figure 7.** Total porosity accessible to water a) versus the drying temperature used and b) versus the volume of
 310 water introduced in the initial geopolymer mixture, for a drying temperature of 105 °C

311

312 For the three W/S mass ratios, the initial water volume introduced into the mixture was
 313 calculated, then compared to the total pore value (obtained at T_{drying} of 105 °C). These results,
 314 presented in Figure 7b, show a very good correlation, illustrating a direct proportionality
 315 between the volume of water introduced and the final porosity of the geopolymer. So, in

316 addition to confirming that the water in the geopolymer appears to be present mostly as "free
317 water", these results show that the total porosity of a geopolymer can be chosen and fixed
318 before its preparation. Since a linear relationship was also made between the initial amount of
319 water and the mechanical performance (Figure 2 a), it is possible to say that there is a direct
320 correlation between total porosity and mechanical strength. Furthermore , knowing that the
321 porosity has a direct influence on the transfer properties and thus on the durability of the
322 materials, the possibility of choosing its value in advance could be a clear advantage for the
323 development of geopolymer.

324 MIP analysis was performed on GP0.40, GP0.47 and GP 0.56 to evaluate the influence of the
325 water content on the geopolymer porous network microstructure. The relative mercury
326 volume introduced versus the pore access diameter is presented in Figure 8a along with the
327 curve of the relative pore volume versus diameter (Figure 8b). For the geopolymer having a
328 W/S mass ratio of 0.40 it was calculated that 95% of the mercury was introduced for pore
329 diameters of 7 to 20 nm (with 83% between 10 and 20 nm), which shows a homogeneous
330 distribution of the pore access diameter. Thus, when the curve of the relative pore volume
331 versus diameter is observed (Figure 8b), the geopolymer has a single population of pore
332 access centred on a diameter of 13 nm. These results confirm the monomodal nature of the
333 porous network of the geopolymer observed in the literature (Rovnaník 2010, Boher 2014).

334 These figures also show that all three formulations led to monomodal porous networks,
335 whatever the amount of water initially introduced. The cumulative pore volume representation
336 confirmed the increase in total volume measured with water intrusion when the initial water
337 amount increased and its derivative revealed that the pore access diameter also increased.

338

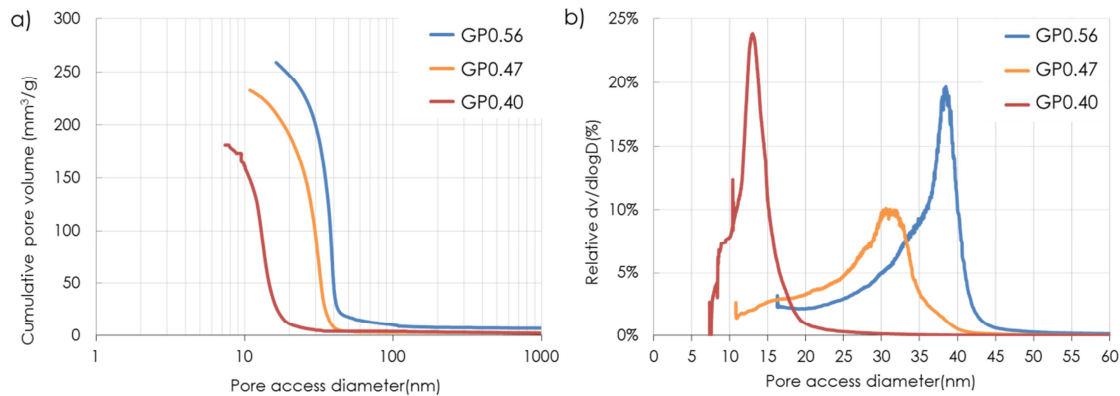


Figure 8. Relative mercury volume introduced and relative pore volume versus pore access diameter for geopolymers GP0.40, GP0.47 and GP0.56.

339
 340
 341
 342
 343
 344
 345
 346
 347
 348
 349
 350
 351
 352
 353
 354
 355
 356
 357
 358
 359
 360
 361

The median pore access diameter therefore increased from 13 nm for GP0.40 to 29 nm for GP0.47 and, finally, 36 nm for GP0.56. When the median diameter increased, the spread of the value also increased, as 90% of the mercury was introduced between 7 and 18 nm for GP0.40, between 11 and 35 nm for GP0.47, and between 16 and 42 nm for GP0.56. The notable difference in pore access diameter between the formulation having the least water and the other two could support the hypothesis made previously on the fact that GP0.40 had such a fine porosity that the evaporation of the "free water" during drying damaged the structure. A study of nitrogen adsorption-desorption isotherms also made on geopolymer GP0.40 provided additional information. The adsorption and desorption isotherms of Figure 9a show a distinct hysteresis loop for relative partial pressure (P/P_0) between 0.8 and 1.0. The passage of the desorption curve below the absorption curve (until P/P_0 of 0.75) was associated with degassing problems during the analysis (degassing temperature of 100 °C). Nevertheless, the closeness of the hysteresis loop at $P/P_0 > 0.40$ and a type IV sorption behaviour with a hysteresis loop of type 1 on a loop of type 2, which have already been identified on metakaolin geopolymer samples by Steins et al. (2013), indicate the absence of micropores and the formation of a well-defined mesoporous texture having interconnected pores with narrow necks and wide voids, called 'ink-bottle pores'. The BJH pore-size distribution (Figure 9b) confirms the monomodal nature of the porous network centred on 15 nm.

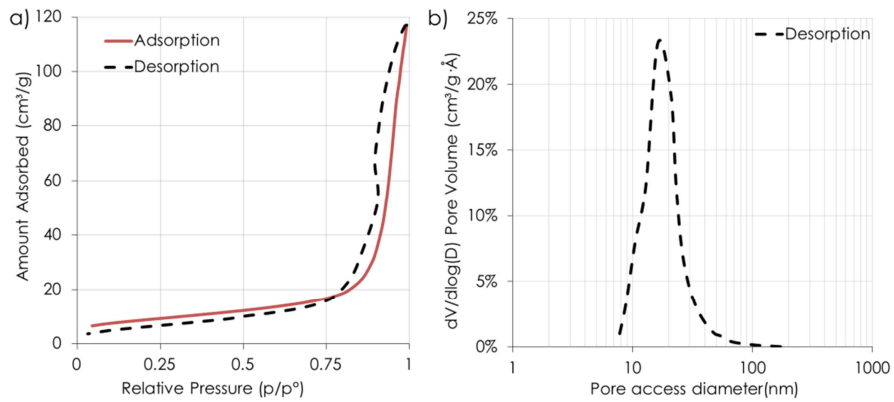


Figure 9. a) Nitrogen adsorption–desorption isotherms and b) BJH pore-size distribution for the GP0.40 geopolymer paste.

362

363

364

365

366

Finally, in order to be able to observe the porosity of a hardened geopolymer clearly, SEM observations were made on a 100 day old GP0.40 section obtained by cutting with the focused ion beam technique. With this cutting of nanometric precision, it is possible to see inside the material without degrading the porous network, as can be seen in Figure 10. It should be noted that the black streaks observed on the SEM images are due to the ion beams used to cut the materials, and the lighter layer at the top of the cross-section corresponds to the platinum depot made to protect the cut out.

372

373

Valuable information can be obtained from these images:

374

- Heterogeneity is clearly observed within the geopolymer in Figure 10a and b as, in addition to the quartz grains recognisable by their well-defined shapes and their grey colour, many cavities are also observed.

375

376

377

- A larger zoom (Figure 10 b) and c)) reveals that these cavities seem to be formed by multiple layers contained within the matrix. The shape, orientation and size of these layers and cavities recall the structure of kaolinite or metakaolinite layers (San Nicolas, 2011). This shows that some of the introduced metakaolin was not fully dissolved by the activating solution during the geopolymerization.

378

379

380

381

382

- In addition to this large layered porosity, the largest zoom (Figure 10d) clearly shows the monomodal mesoporosity of the geopolymer observed during MIP. The many black holes visible in Figure 10d all measure around 10-30 nm and were found in very

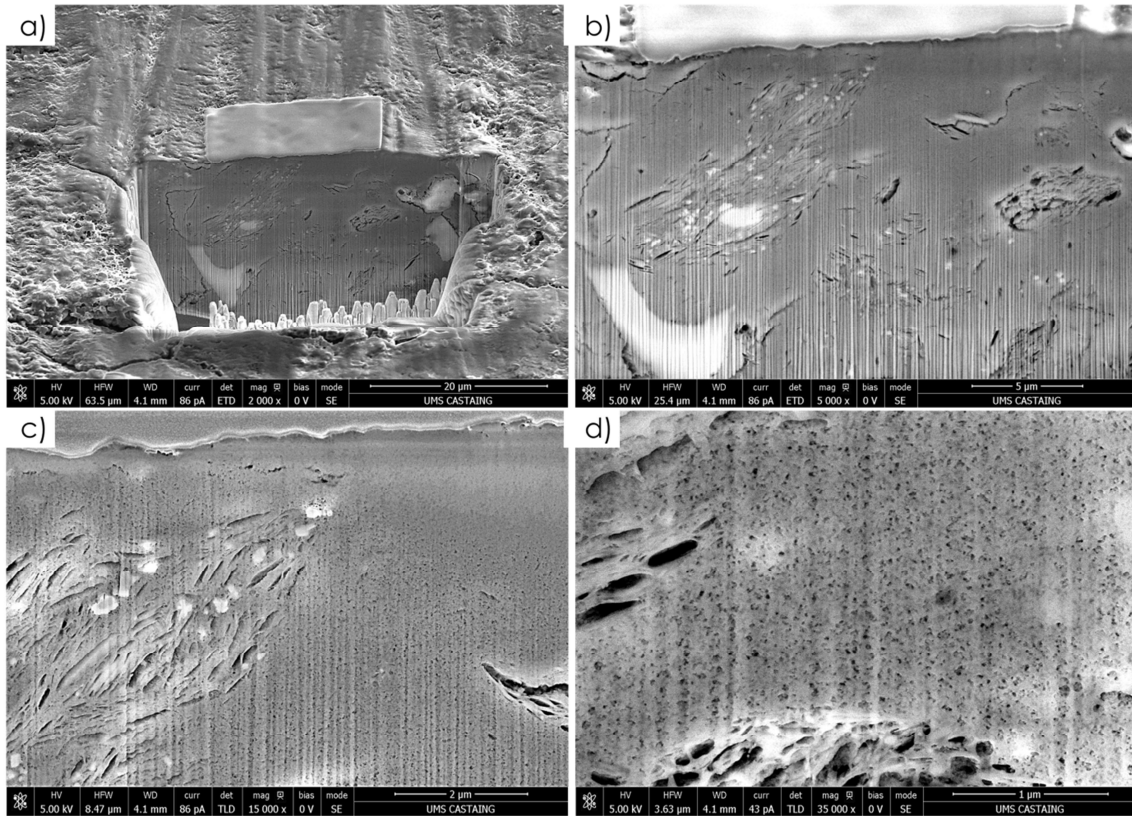
383

384

385 large quantities in the section observed. The presence of these two forms of porosity
386 confirms the presence of the "ink bottle" effect observed by analysis of the results of
387 absorption/desorption of gas.

388 - The observation of this monomodal mesoporosity on this scale, resembling that of a
389 sponge, also confirms the interconnectivity of geopolymer porosity.

390



391

392 **Figure 10.** Electronic scanning microscope images of a cross section of 100 day old geopolymer obtained by
393 focused ion beam a) x2000, b) x5000, c) x10000 and d) x35000
394

395 3.4 Consequences regarding the durability

396 To go further, it is interesting to discuss the direct consequences of these results for the
397 development of geopolymers as construction materials. In the science of building materials,
398 porosity is sometimes considered as a direct indicator of the durability of materials (Baroghel-
399 Bouny, V; 2004). In fact, the porosity is related to the transfer properties of the material,
400 which are responsible for the more or less rapid intrusion of compounds that are harmful to

401 the structure, such as carbon dioxide or chlorides. In view of the large interconnected porosity
402 of metakaolin-based geopolymers, the transfer properties had to be considered. Intrinsic air
403 permeability measurements were performed on geopolymer mortars using the Cembureau
404 apparatus. A very high permeability of 8456.10^{-18} m² was measured after drying at 105 °C.
405 Tests of chloride ion diffusion by migration were also carried out on three geopolymer
406 concrete samples, according to standard NT Build 492. Generally, for cementitious materials,
407 the depth of penetration of chloride ions corresponds to about half of the sample at the end of
408 the test. On geopolymer samples, the chloride ions had completely passed through the test
409 piece at the end of the test (i.e. after 24 h at 10 V) making it impossible to calculate a chloride
410 diffusion coefficient. Thus it seems that the diffusion of chlorides through metakaolin-based
411 geopolymer is much faster than through known materials based on Portland cement and the
412 transfer properties of this geopolymer appear to be unfavourable compared with those of
413 Portland cement. The SEM images obtained (Figure 10) confirm these data by showing a
414 large volume of void in the structure, allowing the transport of air or water. However,
415 comparison with a cement matrix is difficult in view of the great differences in chemical
416 composition between these two materials. A carbonation study previously performed on the
417 same geopolymer material concluded that, although carbonation of the pore solution was
418 extremely rapid in geopolymer, the risks related to the durability of the structure would be
419 limited (Pouhet and Cyr, 2016b). The amount of water initially introduced into the
420 formulation of geopolymers necessarily has a direct influence on the transfer properties of the
421 material and must be taken into account. However, it would be hasty to draw conclusions
422 regarding the consequences on the durability of the structure without further investigations.

423

424 **4. Conclusion**

425 This study has proposed an evaluation of the influence that the amount of water initially
426 introduced has on the hardened properties a geopolymer mixture with a fixed formulation.
427 The conclusions drawn and the consequences that can be expected regarding the development
428 and the durability of geopolymer are listed below.

429 Increasing the amount of initial water in the mixture significantly reduces the mechanical
430 performance measured at 7 days. It seems that this decrease follows a linear trend, which
431 implies that the final performance can be anticipated as soon as the water content is known.
432 However, this also implies that great caution must be taken during the fabrication of
433 geopolymer, especially in large quantities, as a small error in the mass of water introduced
434 may result in a significant variation in the final mechanical performance. That being said, a
435 very wide range of applications seem possible for geopolymers, particularly in the field of
436 construction, as they develop significant mechanical performance in just seven days with a
437 range of water content traditionally used in construction materials.

438 The investigation of the bonded water during geopolymerization led to the conclusion that
439 more than 90% of the water introduced would be "free water", which is easily removable, and
440 therefore would not contribute to the stiffness of the material. The water present in the
441 hardened geopolymer porosity would thus have no influence regarding the mechanical
442 performance of the material. This water could be largely withdrawn, which could be useful
443 for certain applications such as refractory materials. However, it should be noted that the
444 departure of this pore water can in some cases be detrimental to the structure and lead to a
445 decrease in strength.

446 The porosity studies reported here show a pore volume for the geopolymer paste that is large
447 but in agreement with the literature. It appears that the total volume of the geopolymer pores
448 is proportional to the volume of water initially introduced in the mixture, which is consistent
449 with the conclusion of the bonded water study presented in this paper. The quantity of water
450 introduced thus makes it possible to fix the final pore volume, and also the mean diameter of
451 the mesoporosity. The transfer properties measured in this study are in agreement with the
452 large porosity observed for the geopolymer, but further investigations on the durability must
453 be carried out before drawing conclusions on the long term behaviour of these materials.

454

455 **Acknowledgments**

456 The authors are very grateful to SEAC Guiraud and the Association Nationale de la
457 Recherche Technique (ANRT) for supporting the present research. Argeco Developpement
458 and Woellner are also acknowledged for their material support. The quality of the assistance
459 provided at the Raimond Castaing microscopy structure and the CIRIMAT are also
460 acknowledged.

461 **References**

- 462 Álvarez-Ayuso, E., Querol, X., Plana, F., Alastuey, A., Moreno, N., Izquierdo, M., ... & Barra, M. (2008).
463 Environmental, physical and structural characterisation of geopolymer matrixes synthesised from coal
464 (co-) combustion fly ashes. *Journal of Hazardous Materials*, 154(1), 175-183.
- 465 Barbosa, V.F.F., MacKenzie, K.J.D. and Thaumaturgo, C. (2000) Synthesis and characterisation of materials
466 based on inorganic polymers of alumina and silica: sodium polysialate polymers. *International*
467 *Journal of Inorganic Materials*, 2(4): 309-317.
- 468 Baroghel-Bouny, V. (2004). Conception des bétons pour une durée de vie donnée des ouvrages-Maîtrise de la
469 durabilité vis à vis de la corrosion des armatures et de l'alcali-réaction-Etat de l'art et guide pour la mise
470 en oeuvre d'une approche performantielle et prédictive sur la base d'indicateurs de durabilité. *Association*
471 *Française du Génie Civil*.
- 472 Bligh, R., & Glasby, T. (2013). Development of geopolymer precast floor panels for the Global Change Institute
473 at University of Queensland. In *Proceedings Concrete Institute of Australia Biennial Conference*,
474 *Concrete*.
- 475 Boher, C., Martin, I., Lorente, S., Frizon, F. (2014) Experimental investigation of gas diffusion through
476 monomodal materials. Application to geopolymers and Vycor[®] glasses, *Microporous and Mesoporous*
477 *Materials*, 184:28-36.
- 478 Duxson P., Provis, J. L., Lukey, G. C., Mallicoat, S. W., Waltraud, M., Kriven, W., Van Deventer, J.S.J. (2005)
479 Understanding the relationship between geopolymer composition, microstructure and mechanical
480 properties, *Colloids and Surfaces A: Physicochemical and Engineering Aspects*, 269(1-3): 47-58 DOI:
481 10.1016/j.colsurfa.2005.06.060.
- 482 Duxson P., Fernández-Jiménez, A., Provis, J. L., Lukey, G. C., Palomo, A., Deventer, J. S. J., (2007a)
483 Geopolymer technology: the current state of the art. *Journal of Materials Science*, 42(9): 2917-
484 2933.
- 485 Duxson P., Mallicoat, S. W., Lukey, J. L., Kriven, W., Van Deventer, J.S.J. (2007b), The effect of alkali and
486 Si/Al ratio on the development of mechanical properties of metakaolin-based geopolymers. *Colloids and*
487 *Surfaces A: Physicochemical and Engineering Aspects*. 292(1): 8-20.
- 488 Kamaloo, A., Ganjkanlou, Y., Aboutalebi, S. H., and Nouranian H. (2010) Modeling of compressive strength
489 of metakaolin based geopolymers by the use of artificial neural network. *International Journal of*
490 *Engineering*, 23(2):145-152.

491 Lizcano, M., Gonzalez, A., Basu, S., Lozano, K., & Radovic, M. (2012). Effects of Water Content and Chemical
492 Composition on Structural Properties of Alkaline Activated Metakaolin-Based Geopolymers. *Journal of*
493 *the American Ceramic Society*, 95(7), 2169-2177.

494 Okada, K., Ooyama, A., Isobe, T., Kameshima, Y., Nakajima, A., & MacKenzie, K. J. (2009). Water retention
495 properties of porous geopolymers for use in cooling applications. *Journal of the European Ceramic*
496 *Society*, 29(10), 1917-1923.

497 Pacheco-Torgal, F., Labrincha, J., Leonelli, C., Palomo, A., & Chindaprasit, P. (Eds.). (2014). Handbook of
498 alkali-activated cements, mortars and concretes. Elsevier.

499 Palomo, A., Krivenko, P., Garcia-Lodeiro, I., Kavalerova, E., Maltseva, O., & Fernández-Jiménez, A. (2014). A
500 review on alkaline activation: new analytical perspectives. *Materiales de Construcción*, 64(315), e022.

501 Park, S., & Pour-Ghaz, M. (2018). What is the role of water in the geopolymerization of metakaolin?.
502 *Construction and Building Materials*, 182, 360-370.

503 Perera, D. S., Vance, E. R., Finnie, K. S., Blackford, M. G., Hanna, J. V., & Cassidy, D. J. (2005). Disposition of
504 water in metakaolinite based geopolymers. *Advances in Ceramic Matrix Composites XI, Volume 175*,
505 225-236.

506 Pouhet, R. (2015). *Formulation and durability of metakaolin-based geopolymers* (Doctoral dissertation,
507 Université de Toulouse, Université Toulouse III-Paul Sabatier).

508 Pouhet, R. and Cyr, M. (2016a). Formulation and performance of flash metakaolin geopolymer concretes.
509 *Construction and Building Materials*, 120, 150-160.

510 Pouhet, R. and Cyr, M. (2016b). Carbonation in the pore solution of metakaolin-based geopolymer. *Cement and*
511 *Concrete Research*, 88, 227-235.

512 Provis, J. L., and Van Deventer, J. S. J. (2009a), Geopolymers: Structures, Processing, Properties and Industrial
513 Applications, *Woodhead Publishing Limited*.

514 Provis, J. L., Yong, C. Z., Duxson, P., & van Deventer, J. S. (2009b). Correlating mechanical and thermal
515 properties of sodium silicate-fly ash geopolymers. *Colloids and Surfaces A: Physicochemical and*
516 *Engineering Aspects*, 336(1), 57-63.

517 Rovnaník, P. (2010) Effect of curing temperature on the development of hard structure of metakaolin-based
518 geopolymer, *Construction and Building Materials*, 24(7): 1176-1183.
519 DOI:10.1016/j.conbuildmat.2009.12.023.

520 Rowles, M., et O'Connor, B. (2003) Chemical optimisation of the compressive strength of aluminosilicate
521 geopolymers synthesised by sodium silicate activation of metakaolinite. *Journal of Materials*
522 *Chemistry* 13(5): 1161-1165. DOI:10.1039/b212629j.

523 San Nicolas, R. (2011). *Approche performantielle des bétons avec métakaolins obtenus par calcination*
524 *flash* (Doctoral dissertation, Université Toulouse III-Paul Sabatier).

525 San Nicolas, R., Cyr, M., Escadeillas G. (2013) Characteristics and applications of flash metakaolins, *Applied*
526 *Clay Science*, 83–84: 253-262. DOI: 10.1016/j.clay.2013.08.036.

527 Shi, C., Krivenko, P. v. and Roy, D. M. (2006) *Alkali-Activated Cements and Concretes*, Abingdon, UK, Taylor
528 and Francis.

- 529 Steins, P., Poulesquen, A., Frizon, F., Diat, O., Jestin, J., Causse, J., Lambertina, D., Rossignol, S. (2013) Effect
530 of aging and alkali activator on the porous structure of a geopolymer, *Journal of Applied Crystallography*,
531 47:316-324.
- 532 White, C. E., Provis, J. L., Proffen, T., & Van Deventer, J. S. (2010). The effects of temperature on the local
533 structure of metakaolin-based geopolymer binder: A neutron pair distribution function investigation.
534 *Journal of the American Ceramic Society*, 93(10), 3486-3492.
- 535 Zuhua, Z., Xiao, Y., Huajun, Z., & Yue, C. (2009). Role of water in the synthesis of calcined kaolin-based
536 geopolymer. *Applied Clay Science*, 43(2), 218-223.